OXFORD

ORIGINAL ARTICLE

Molecular and biochemical alterations in tubular epithelial cells of patients with isolated methylmalonic aciduria

T. Ruppert[1], A. Schumann[1,2,3,4], H.J. Gröne[5], J.G. Okun[1], S. Kölker[1], M.A. Morath[1] and S.W. Sauer[1,*]

[1]Department of General Pediatrics, Division of Neuropediatrics and Metabolic Medicine, University Children's Hospital Heidelberg, D-69120 Heidelberg, Germany, [2]Division of Metabolism and Children's Research Center, University Children's Hospital, Zurich, Switzerland, [3]Institute of Physiology, [4]Center for Integrative Human Physiology, University of Zurich, Zurich, Switzerland and [5]Department of Cellular and Molecular Pathology, German Cancer Research Center (DKFZ), Heidelberg, Germany

*To whom correspondence should be addressed. Tel: +49 62215637399; Fax: +49 6221566391; Email: sven.sauer@med.uni-heidelberg.de

Abstract

Methylmalonic acidurias (MMAurias) are a group of inherited disorders in the catabolism of branched-chain amino acids, odd-chain fatty acids and cholesterol caused by complete or partial deficiency of methylmalonyl-CoA mutase (mut^0 and mut^- subtype respectively) and by defects in the metabolism of its cofactor 5′-deoxyadenosylcobalamin (*cblA*, *cblB* or *cblD* variant 2 type). A long-term complication found in patients with mut^0 and *cblB* variant is chronic tubulointerstitial nephritis. The underlying pathomechanism has remained unknown. We established an *in vitro* model of tubular epithelial cells from patient urine (hTEC; 9 controls, 5 mut^0, 1 *cblB*). In all human tubular epithelial cell (hTEC) lines we found specific tubular markers (AQP1, UMOD, AQP2). Patient cells showed disturbance of energy metabolism in glycolysis, mitochondrial respiratory chain and Krebs cycle in concert with increased reactive oxygen species (ROS) formation. Electron micrographs indicated increased autophagosome production and endoplasmic reticulum stress, which was supported by positive acridine orange staining and elevated levels of LC3 II, P62 and pIRE1. Screening mTOR signaling revealed a release of inhibition of autophagy. Patient hTEC produced and secreted elevated amounts of the pro-inflammatory cytokine IL8, which was highly correlated with the acridine orange staining. Summarizing, hTEC of MMAuria patients are characterized by disturbed energy metabolism and ROS production that lead to increased autophagy and IL8 secretion.

Introduction

Methylmalonic acidurias (MMAurias) are an etiologically heterogeneous group of inherited disorders in the catabolism of L-isoleucine, L-valine, L-methionine and L-threonine as well as odd-chain fatty acids and cholesterol with an cumulative prevalence of 1:50 000–1: 100 000 newborns ([1]). Isolated MMAurias are caused by complete or partial deficiency of the mitochondrial enzyme methylmalonyl-CoA mutase catalyzing the conversion of methylmalonyl-CoA to succinyl-CoA (MCM; EC 5.4.99.2; mut^0 enzymatic subtype or mut^- subtype, respectively), or by defects in the uptake, transport or synthesis of its cofactor 5′-deoxyade-nosylcobalamin (*cblA*, *cblB* or *cblD* variant 2 type). Affected individuals display elevated levels of methylmalonic acid (MMA), propionate, 3-hydroxypropionate and 2-methylcitrate in tissues and body fluids ([2]). Neonatal sepsis-like metabolic crisis after a short symptom-free period may be the first and life-threatening

manifestation of MMAurias (2). Recurrent acute metabolic crises are often triggered by catabolic state, e.g. due to febrile illness. Major long-term complications are neurological impairment (3,4) and chronic tubulointerstitial nephritis (cTIN) with progressive impairment of renal function (5). Patients with mut[0] and cblB defects bear the highest risk to develop cTIN (5). Severe disturbance of mitochondrial energy metabolism due to synergistic action of accumulating toxic metabolites, in particular propionyl-CoA, has been suggested to underlie neurodegenerative changes (6). Little is known about the pathomechanism of renal disease. $Mcm^{-/-}$ mice only survive 48 h after birth limiting investigation of long-term complications (7). Stable expression of Mcm in the liver of $Mcm^{-/-}$ mice has recently been shown to rescue neonatal lethality but does not prevent renal dysfunction (8). Proximal tubular cells of these mice displayed enlarged mitochondria with disorganized cristae indicating mitochondrial dysfunction, decreased glomerular filtration rate, but no clear signs of inflammation or cTIN were reported. Similar morphological changes have been described in patients (9), however combined with infiltration of immune cells. Therefore, the renal phenotype of the existing mouse models rather resembles tubular atrophy. Interestingly, it has been found that the pattern of excreted cells in the urine correlates with the progression nephritis (10). To gain further insight in the renal pathogenesis we therefore established and characterized an *in vitro* model of tubular epithelial cells gained from urine of affected patients. As additional controls we used tubular epithelial cells from propionic aciduria (PAuria) patients. This disease is caused by deficiency of the enzyme propionyl-CoA carboxylase catalyzing the decarboxylation of propionyl-CoA to methylmalonyl-CoA and, therefore, lying one enzymatic step before MCM. Importantly, PAuria patients display neurological disease and myopathies but do not typically develop cTIN.

Results

Characterization of human proximal tubule cells

We purified human tubular epithelial cells (hTEC) from 9 healthy controls (Co_1–9), 3 PAuria patients (PA_1–3), 5 mut[0] patients (mut[0]_1–5) and one cblB patient (cblB_1). Since cblB patients have the same risk to develop cTIN (5) and hTEC of the latter patient did not differ from hTEC of mut[0] in any of the performed experiments, we combined both disease subtype under MMAuria patients for data analysis in the text and refer to 'mut' in figures due to space limitations. All included mut[0] patients showed increased creatinine clearance as well as elevated MMA concentrations in urine and plasma (data not shown). Age range of controls was between 3 and 37 years, mut[0] patients ranged between 11–40 years and PA patients between 1 and 7 years (Table 1).

Next, hTEC were tested for expression of specific marker proteins for different kidney segments. Supplementary Material, Figure S1 shows representative immunoblots for these markers (AQP1, UMOD, AQP2) and MCM. hTEC from control and patients with MMAurias express markers of the proximal and distal tubule as well as of the thick ascending limb. A high expression of Mcm is observed in control cells. In mut[0]_1, 2 we could not detect MCM, whereas mut[0]_3, 5 and cblB_1 show reduced expression. This is probably due to the fact that the anti-MCM antibody recognizes the whole enzyme, thus may interact with parts of non-functional enzyme present in these cells. The cells derived from healthy controls and MMAuria patients were investigated for MCM activity using ^{14}C incorporation assay confirming the enzymatic defect (data not shown). Stimulation with

Table 1. Included MMAuria patients

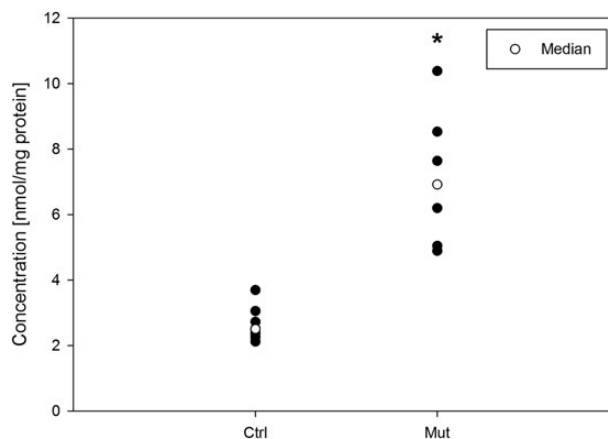| hTEC	Age	Mutation	MMA in plasma (μM)
mut[0]_1	22	T862C, T862C	4112 (±1430)
mut[0]_2	23	C982T, C982T	4239 (±2845)
mut[0]_3	18	G607A, G607A	1230 (±414)
mut[0]_4	11	G607A, C1105Ts	3278 (±1527)
mut[0]_5	16	T862C, A1157G	4579 (±1527)
cblB_1	40	C556T, Arg186W	3143 (±453)

Figure 1. Characterization of hTEC. In line with their genotype, hTEC of MMAuria patients displayed elevated MMA production compared with control cells. Data are presented as dot plots, ctrl $n = 9$, mut $n = 6$ *$P < 0.05$.

adenosylcobalamin showed that all mut[0] cell lines are unresponsive to cofactor stimulation (data not shown). Consistently, MMAuria patient hTEC showed increased MMA secretion (Fig. 1).

Summarizing, hTEC lines gained from human urine express characteristic markers of tubular epithelial cells. Further, MMAuria patient cell lines display the corresponding enzymatic and metabolic phenotype.

Profiling energy metabolism

As disturbance of energy metabolism is thought to play a major role in the pathogenesis of MMAurias, we assessed cellular energy homeostasis in hTEC on various levels. First, we determined mitochondrial respiration in DMEM+10% FCS and Krebs Ringer buffer (KRB) pyruvate (5 mM) to directly stimulate mitochondrial respiration. hTEC of PA and MMAuria patients displayed decreased mitochondrial respiration in standard medium, whereas only cells of MMAuria patients revealed a diminished ability to respire on pyruvate (Fig. 2A). It has been previously shown that the metabolite propionyl-CoA accumulating in PA and MMAuria inhibits pyruvate and 2-oxoglutarate dehydrogenase complex (11). Therefore we measured the mitochondrial pyruvate and 2-oxoglutarate catabolism by radiometric analysis. hTEC of PA patients showed a decreased ^{14}C-CO_2 production from pyruvate, whereas 2-oxoglutarate catabolism was slowed in cells from MMAuria patients (Fig. 2B). Next, we analyzed energy metabolism on the level of single enzymes, i.e. respiratory chain and glycolysis. Of note, phosphofructokinase (PFK1) activity was specifically reduced in hTEC of MMAuria patients (Fig. 2C). Lactate dehydrogenase activity was increased in these cells. Next we aimed to determine activity of respiratory chain complexes,
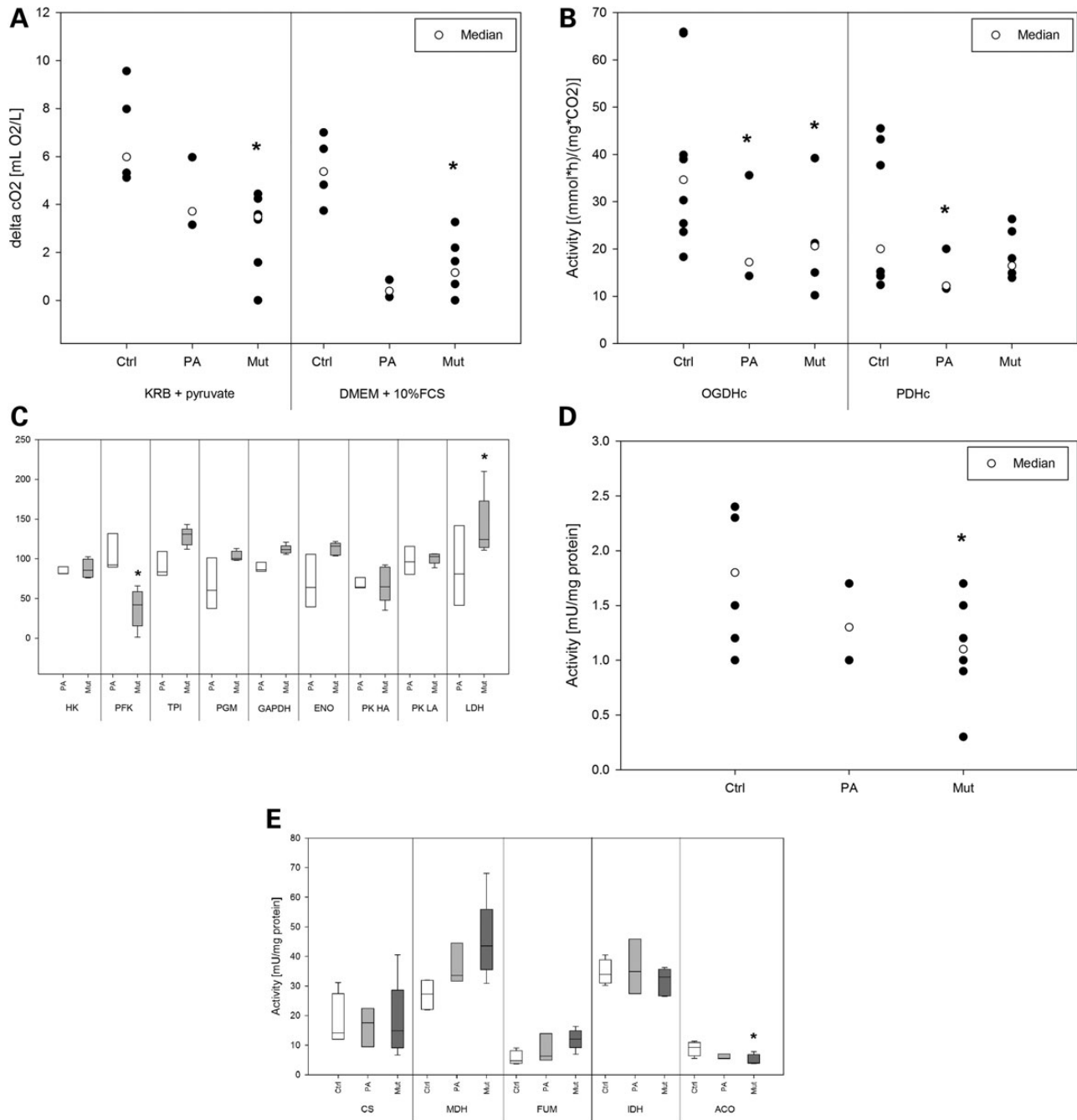
Figure 2. Dysfunction of energy metabolism. To assess energy metabolism in hTEC we performed metabolic flux experiments and recorded single enzyme activities of major pathways in control cells as well as hTEC of MMAuria and PAuria patients. (**A**) First, we analyzed mitochondrial respiration standard DMEM and KRB+4 mM pyruvate. hTEC of MMAuria and PAuria patients displayed reduced mitochondrial respiration in DMEM, whereas only MMAuria patient hTEC had a lower oxygen consumption on the substrate pyruvate. In line with this finding, (**B**) both patient cell lines revealed a reduced ^{14}CO production on the substrate ^{14}C-2-oxoglutarate, but break down of ^{14}C-pyruvate was only altered in PAuria hTEC. (**C**) Analysis of single enzymes of glycolysis (HK: hexokinase; PFK: phosphofructokinase; TPI: triose phosphate isomerase; GAPDH: glyceraldehydphosphat-dehydrogenase; PGM: phosphoglycerate mutase; E: enolase; PK HA: pyruvate kinase M2 tetramer; PK LA: pyruvate kinase M2 dimer; LDH: lactate dehydrogenase) showed a strongly diminished PFK and an increase of LDH activity in hTEC of MMAuria patients. Adding to the finding of disturbed mitochondrial energy metabolism in these cell lines, we found a reduction of cytochrome c oxidase (**D**) and aconitase (**E**; CS, citrate synthase; MDH, malate dehydrogenase, FUM, fumarase; IDH, isocitrate dehydrogenase; ACO, aconitase). Data are presented as dot plots (A, B and D) or box plots (C and E), ctrl $n = 5$, PA $n = 3$, mut $n = 6$ * $P < 0.05$.

but we failed to gain mitochondrial preparations from hTEC of MMAuria patients. We tested different systems for cell homogenization (disruption with needles of different gauges, various Potter-Elvehjem homogenizers) and subcellular fractionation techniques (differential centrifugation versus density gradient centrifugation), but we were not able to achieve a sufficient quality and quantity of mitochondrial enrichment. To circumvent the need of mitochondrial fraction, we used digitonin permeabilized cells to record respiratory chain complex activities (12). In line with the notion of decreased mitochondrial respiration due to

disturbed integrity of mitochondrial membranes, cytochrome *c* oxidase activity was diminished in hTEC of MMAuria patients (Fig. 2D).

Using this approach we also determined activity of citrate cycle enzymes. In hTEC of MMAuria patients we found decreased activity of aconitase (Fig. 2E). Other investigated proteins of citrate cycle were unchanged in their activity.

Generation of reactive oxygen species

Oxidative stress is commonly found in conditions of disturbed energy metabolism, particularly involving the respiratory chain. First, we evaluated glutathione status as a general marker

of increased reactive oxygen species (ROS) generation. hTEC of MMAuria patients indeed showed decreased levels of reduced and increased levels of oxidized glutathione (Fig. 3A). Next, we used H_2DCFDA staining and FACS analysis to measure the actual ROS generation (Fig. 3B). Cells were cultivated in KRB and energy substrates (glucose, pyruvate or glutamine) in the presence or absence of PA, MMA and isoleucine. Regardless of the supplied substrate, hTEC of MMAuria patients generated more ROS than control cells or PA patient cells. Incubation of MMAuria cells in Williams′ medium E which is enriched with anti-oxidative agents (i.e. glutathione, ascorbic acid) did reduce ROS production compared with the condition KRB + pyruvate stimulating mitochondrial activity ($P = 0.03$).
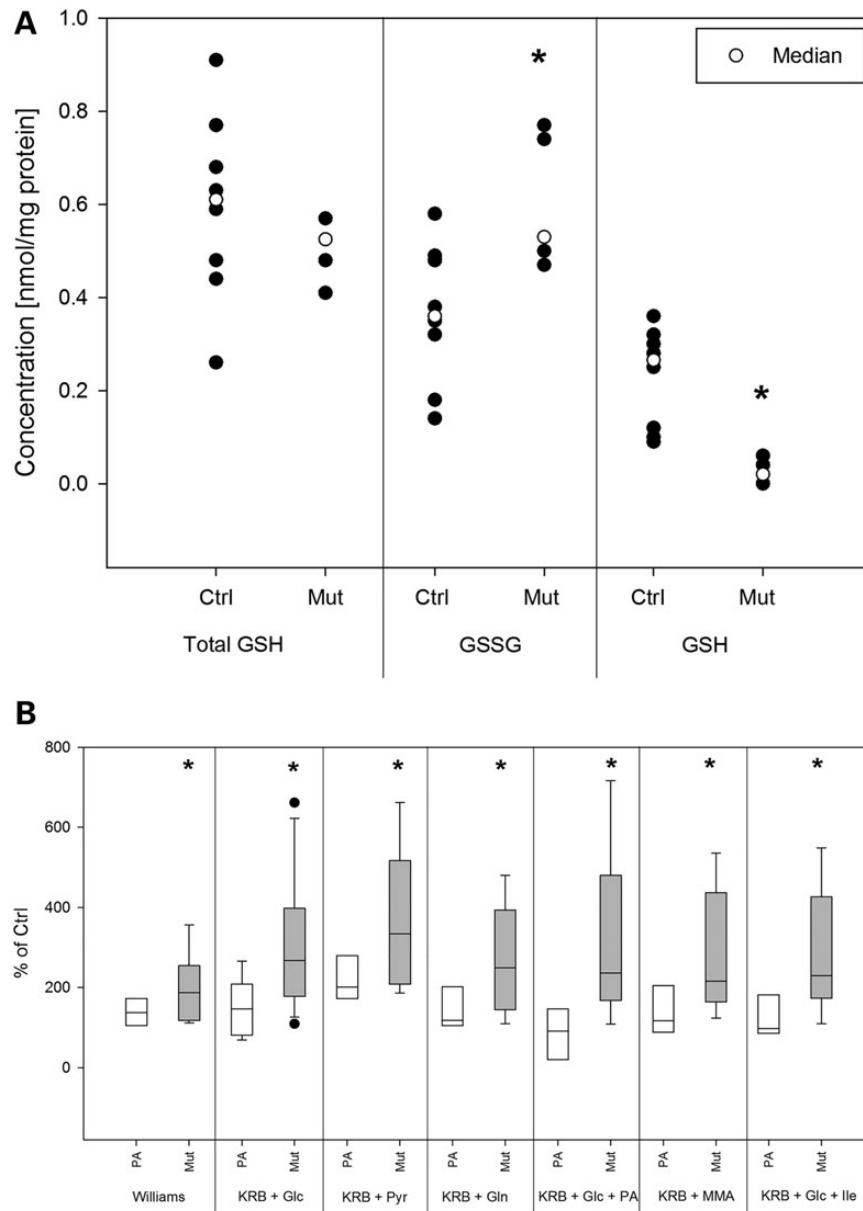

Figure 3. Oxidative stress in hTEC of MMAuria patients. Oxidative stress and ROS production were investigated by analyzing glutathione status (**A**) as well as by the ROS sensitive dye H_2DCFDA (10 µM, (**B**). Total glutathione content was unchanged in hTEC of MMAuria patients, but the amount of oxidized glutathione (GSSG) was increased and the level of reduced glutathione (GSH) diminished in these cells. FACS analyses with H_2DCFDA stained cells showed increased formation of ROS in hTEC of MMAuria patients in all tested conditions, i.e. Williams E medium, KRB supplemented with glucose (Glc), pyruvate (Pyr), glutamine (Gln), propionic acid (PA), MMA or isoleucine (Ile; each 5 mM). Data are presented as dot plots (A) or box plots (B), ctrl $n = 5$, PA $n = 3$, mut $n = 6$ *$P < 0.05$*.
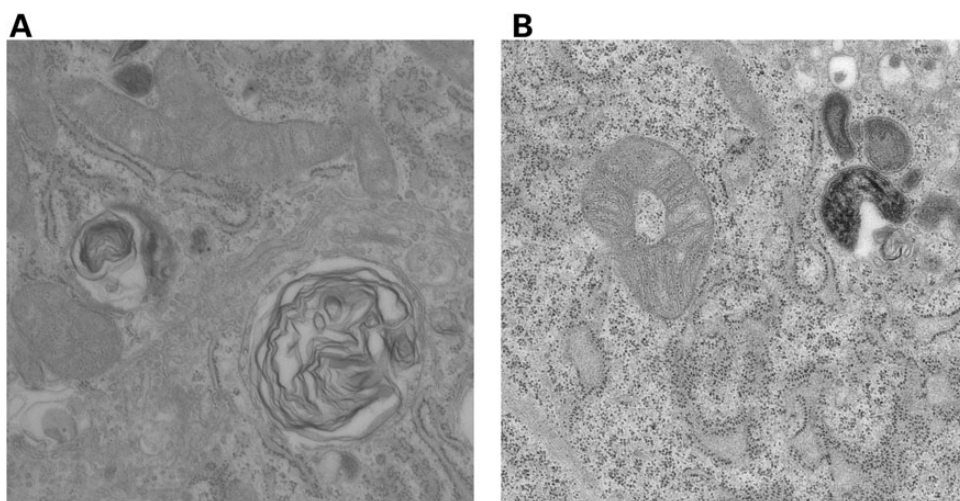
Figure 4. Alterations in ultrastructure. Electron micrographs of all mut^0 hTEC provided indication of increased autophagy and ER stress. Figure 4 shows representative electron micrographs of mut^0_1. Patient hTEC display an increased number of lamellar bodies (**A**) as well as bloated and disarranged ER structures (**B**) indicative of autophagic processes and ER stress respectively.

Induction of autophagy

Electron micrographs of hTECs showed lamellar bodies and dilated endoplasmic reticulum (ER) indicative of autophagic changes and ER stress respectively (Fig. 4). To this end we stained hTEC with acridine orange and analyzed the amount of green fluorescing cells (staining of autophagosomes) by FACS analysis. MMAuria patient cells displayed elevated green staining indicating enhanced autophagic processes (Fig. 5A). Moreover, increased levels of the autophagy marker proteins LC3 II and p62 in these cells corroborate the rise in autophagosomes (Fig. 5B) which was not found in hTEC of PA patients (Fig. 5C). Application of rapamycin as control experiment led to strong induction of autophagy and increased levels of LC3 II and p62.

mTOR complex is a master regulator of autophagy and itself tightly regulated by the energetic state of the cell and nutrient availability, most importantly branched-chain amino acids (13). Of note, the final degradation pathway of the latter is interrupted in MMAuria due to the defect of MCM. To stimulate the mTOR pathway and its response to nutritional signals we cultivated hTEC under low protein conditions, i.e. 0.5 and 1% FCS, and high protein conditions, i.e. 20% FCS. In MMAuria patients the recommended therapeutic regiment aims to reduce the daily protein intake which is a major risk factor for metabolic decompensation. We studied the levels of mTOR, Phospho-mTOR (Ser2448), Phospho-Raptor (Ser792) PRAS40, Phospho-PRAS40 (Thr246), RagC in hTEC of MMAuria as well as PA patients relative to control cells used in the same experiments. Phospho-Raptor and RagC levels remained unchanged in hTEC of MMAuria and PAuria patients (data not shown), whereas MUT-deficient cells responded to an increasing protein load with decreasing ratios of Phospho-mTOR to mTOR as well as of Phospho-PRAS40 to PRAS40 (Fig. 5D). Decreasing phosphorylation level of these proteins reverses the inhibition of autophagy by mTOR complex. Neither hTEC of healthy donors nor of PAuria patients (Fig. 5E) showed this pattern of mTOR regulation. Next, we examined whether the pro-autophagic modulation of mTOR complex by protein loading is associated with increased LC3 II und p62 levels. hTEC of MMAuria patients were indeed characterized by elevated levels of these proteins when media were supplemented with 20% FCS (Fig. 5B). Decreasing FCS concentrations to 1 and 0.5%

abolished this effect and MCM-deficient cells were undistinguishable from control cells. Again, hTEC of PAuria patients responded to this treatment like control cells confirming the specificity of our results (Fig. 5C). AMPK is a key sensor for the cellular energetic state and modulates mTOR activation. However, we could not find increased phosphorylation of AMPK in hTEC of MMAuria or PAuria patients (data not shown).

As a sensor of ER stress we studied the ER transmembrane protein phosphorylated inositol requiring enzyme 1α (pIRE1) again under different FCS conditions (0.5, 1, 20%) revealing an increase in pIRE1 (Fig. 5B) in MUT-deficient cells but not in hTEC of PAuria patients (Fig. 5E).

Inflammatory phenotype

Disturbance of renal tubular energy metabolism is commonly associated with Fanconi syndrome due to lack of energy for tubular transporter. Interestingly, MMAuria patients directly develop cTIN despite impaired energy homeostasis. To gain more insight in the underlying mechanism, we aimed to describe inflammatory molecules generated by patient hTEC. We used a Mix-N-Match ELISArray Kits (SABiosciences) for major cytokines released by the proximal tubule, i.e. IL8, MCP1, MIP-1a, MIP-1b, RANTES, TGF-ß. In addition, we analyzed the expression of several receptors of the complement system CD55, CD46, CD59, CD88 by FACS. Whereas the latter receptors remained unchanged, the Mix-N-Match ELISArray indicated elevated production and secretion of IL8 in hTEC of MMAuria patients (data not shown). Using a quantitative IL8 ELISA (Eli-pair Kit, abcam) we determined the amount of this cytokine secreted to the apical and basolateral site of 12-well Transwell plate as well as its intracellular concentration. Our experiments confirmed that MMAuria hTEC produced and secreted more IL8 than control or PAuria patient hTECs (Fig. 6).

Discussion

To investigate the molecular mechanisms of cTIN in MMAurias, we established tubular epithelial cell lines (hTEC) from affected patients as well as control cell lines from healthy donors and PAuria patients. Molecular characterization of these cells
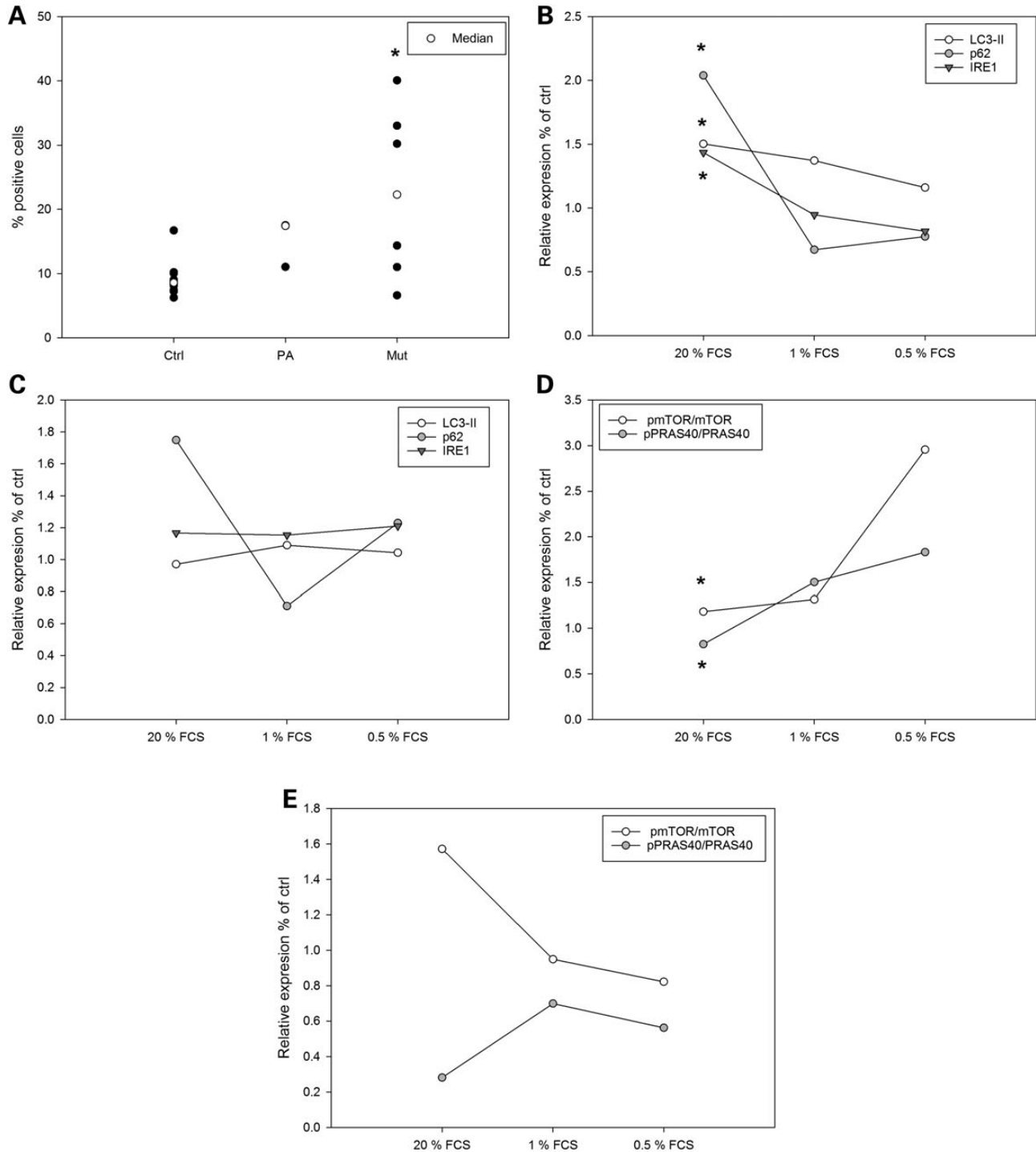
Figure 5. Autophagy and regulation of mTOR. Specifically hTEC of MMAuria patients showed an increased staining with acridine orange indicating elevated autophagy (**A**). Since autophagy and mTOR are regulated by the energetic status of the cell, we cultured hPTEC in DMEM supplemented with 0.5, 1 or 20% to simulate low and high protein/ nutritional energy levels. Elevation of FCS content in medium resulted in an up-regulation of LC3 II and p62 levels (**B**) as well as in a down-regulation of the ratios of phosphorylated to unphosphorylated mTOR and phosphorylated to unphosphorylated PRAS40 (**D**) in hTEC of MMAuria patients. Moreover, increased pIRE1 levels under high FCS conditions indicated ER stress (**B**). Similar patterns for alterations in autophagy and ER stress response (**C**) as well as mTOR signaling (**D**) were not found in hTEC from PAuria patients. Data are presented as dot plots (**A**) or mean (**B–E**), ctrl $n = 5$, PA $n = 3$, mut $n = 6$ *$P < 0.05$.

revealed expression of specific marker proteins of the proximal and distal tubules as well as thick ascending limb to a similar degree in all cell lines. It has previously been shown that the pattern of excreted cells in the urine correlates with the progression nephritis ([10]). Therefore, our hTEC model disease state and damaged area of tubule of the corresponding patients.

Dysfunction of energy metabolism and ROS production

It has previously been shown that in MMAuria and PAuria accumulating metabolites can directly inhibit energy metabolism ([11],[14],[15]). To evaluate overall energy metabolism in hTEC, we measured mitochondrial oxygen consumption in standard
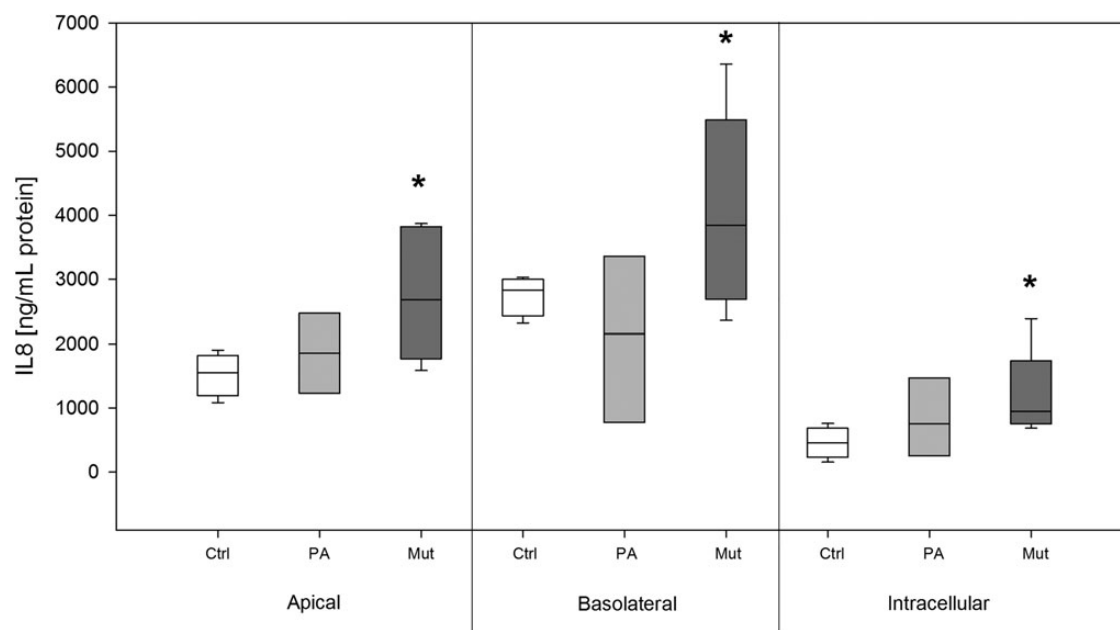
Figure 6. Production and secretion of IL-8. We detected intracellular content as well as secretion to the apical and basolateral compartment of IL8. Only hTEC of MMAuria patients showed increased production and release of this cytokine. Data are presented as box plot, ctrl $n = 5$, PA $n = 3$, mut $n = 6$ *$P < 0.05$*.

DMEM and KRB including pyruvate. hTEC of PAuria and MMAuria patients showed a strong decrease of mitochondrial respiration in DMEM, whereas this decrease was only found for hTEC of MMAuria patients in KRB including pyruvate. Further enzymatic analysis showed decreased activity of PFK1, mitochondrial aconitase, OGDHc and cytochrome *c*-oxidase. PFK1 is a rate limiting enzyme of glycolysis highly regulated by ATP, ADP, AMP, citrate and fructose 2,6-bisphosphate. Of note, we found that 2-methylcitrate is a strong PFK inhibitor (1 mM ~80% reduction of enzyme activity). Since citrate allosterically inhibits PFK, the observed decrease of PFK activity can be caused by accumulating 2-methylcitrate in hTEC. Alternatively, Tp53-induced glycolysis and apoptosis regulator (TIGAR) has been shown to block PFK activity in ischemic proximal tubules to protect these from energy depletion and apoptotic cell death ([16]).

The reduction of mitochondrial respiration as well as cytochrome *c*-oxidase activity in concert with the observed fragility of mitochondria strongly hints to a defect in mitochondrial membrane composition. Of note, the same phenomenon was observed in the attempt to purify mitochondria from Mut-deficient mice ([17]). Reduced activity of cytochrome *c*-oxidase ([18]) or even of all respiratory chain complexes ([9]) has been found in kidney biopsies from MMAuria. Taken together these findings suggest that mitochondrial integrity is altered in MMAuria.

The mitochondrial enzymes aconitase bears metal ions in its catalytic center making it highly sensitive to ROS ([19]) and, consequently, its reduced activity in hTEC of MMAuria patients was indicating increased ROS production. In line with this notion hTEC of MMAuria patients showed increased levels of glutathione disulfide and a diminished content of reduced glutathione. Moreover, using the ROS sensitive dye H_2DCFDA ([20]) we could show that hTEC generate indeed more free oxygen radicals.

Increased autophagy in hTEC of MMAuria patients

In electron micrographs of mut-deficient hTEC lamellar bodies indicated increased production of autophagosomes and autolysosomes. Induction of autophagy has been shown to be a cellular response to chronic, metabolic mitochondrial stress in kidney cells ([21]). Indeed, specifically hTEC of MMAuria patients displayed increased levels of LC3 II and p62 under metabolic stress, i.e. high FCS content. Both proteins play a central role in the maturation of the autophagosomes ([22]). Elevation of AO positive stained cells further supports the notion of increased autophagy. mTORC1 is a master regulator of macro-autophagy and a central energy sensor of the cell. Moreover, maintenance and physiological functions of the kidney are critically dependent on mTOR-modulated autophagy ([23]). To investigate activation status and response of mTORC1 to nutritional signals, we cultured hTEC in DMEM supplemented with 0.5, 1 or 20% FCS. Elevation of FCS content in medium resulted in a down-regulation of the ratios of phosphorylated to unphosphorylated mTOR and phosphorylated to unphosphorylated PRAS40 in hTEC of MMAuria patients causing an inactivation of mTORC1 and, thereby, of its inhibition of autophagy ([24–27]).

Interestingly, electron micrographs also displayed bloated ER structures in hTEC of MMAuria patients indicating elevated ER stress. There is growing evidence that mTORC1 and ER stress are linked via the IRE1-JNK pathway ([28]) and that the crosstalk of this two signaling axis may even orchestrate IL8 secretion ([29]). Further, autophagy can be activated by IRE1 and eIF-2a with PERK ([30]). In line with this notion, we found increased content of phosphorylated IRE1a hTEC of MMAuria patients.

Cytokine secretion

Recruitment of immune cells to inflamed tissue and communication at the site of inflammation occurs via cytokines and receptors. Screening for the production and release of relevant cytokines in our hTEC lines, we found elevated IL8 levels in and secretion from cells of MMAuria patients. IL8 plays a central role in chronic kidney disease including different forms of nephritis and has been shown to be released by tubular epithelial cells ([31]). Since cytokine secretion and, thereby, activation of immune cells plays a pivotal role in the development of cTIN, we tested whether mitochondrial dysfunction using cytochrome c oxidase as indicator, ROS indicated by H_2DCFDA staining, or autophagy

indicated by acridine orange staining would predict the extent of IL8 production and secretion. Indeed, we found a high correlation between acridine orange staining and the amount of IL8 produced and secreted by hTEC of MMAuria patients (Fig. 7; IL8 versus ROS production, $R^2 = 0.47$; IL8 versus cytochrome c oxidase, $R^2 = 0.55$).
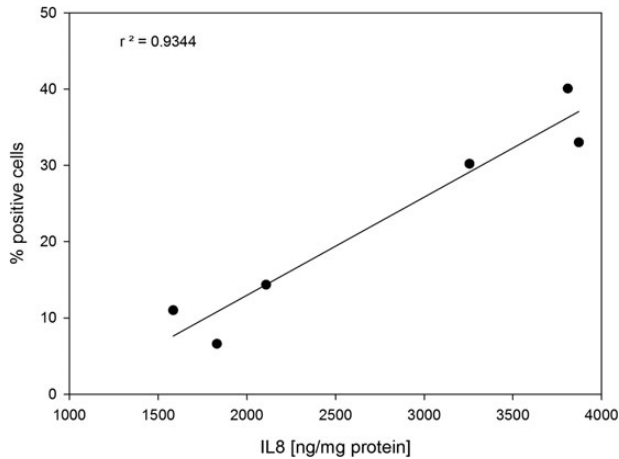

Figure 7. Correlation of IL8 secretion and acridine orange staining. To link the molecular and metabolic alteration, we tested whether there is a correlation between the main findings of our study, i.e. mitochondrial dysfunction, ROS production, autophagy and IL8 secretion. Indeed we found a very high correlation between acridine orange positive stained cells and the extent of secreted IL8.

Figure 8 shows a synopsis of the postulated pathomechanism. Deficiency of MCM leads through a yet unknown mechanism to mitochondrial dysfunction characterized by impaired energy production, ROS generation and loss of mitochondrial integrity. These factors are sufficient to trigger autophagy to clear defect organelles and maintain cellular energy levels. A recent study of Wrobel and colleagues has shown that decreased import of mitochondrial proteins and their subsequent increased cytosolic levels induce unfolded protein response (32). Disturbance of mitochondrial integrity in hTEC of MMAuria patients will result in impaired import of mitochondrial proteins which should accordingly lead via stimulation of unfolded protein response to ER stress. In parallel, dysfunction of cellular energy production releases mTOR-mediated inhibition of autophagy. The interplay of autophagy and ER stress induce production and secretion of IL8.

In summary, our study describes a new *in vitro* model to study the pathomechanism of cTIN in MMAuria consisting of immortalized human, tubular epithelial cells. These cells express specific markers of the proximal and distal tubules as well as the thick ascending limb. We found in hTEC of MMAuria patients severe dysfunction of cellular energy metabolism as well as increased ROS generation and autophagic processes that may lead to increased cytokine (IL8) secretion and development of cTIN.

Materials and Methods

Patient material

The study was performed in accordance with the declaration of Helsinki and was approved by the Institutional Ethics Committee
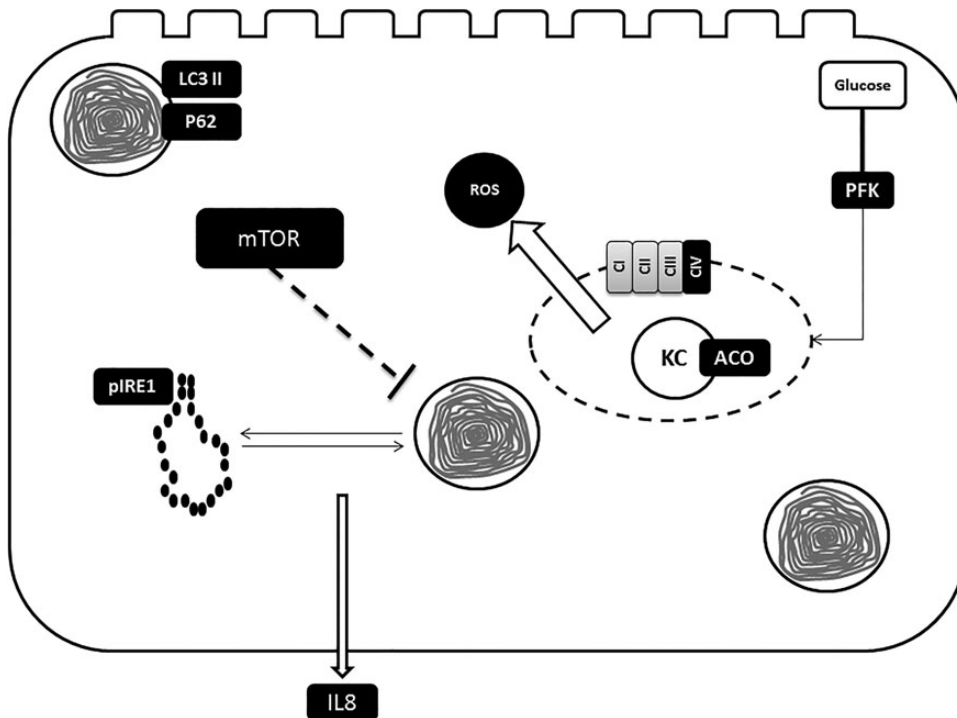

Figure 8. Synopsis of postulated pathomechanism. hTEC of MMuria patients display reduced activities of cytochrome c oxidase (CIV) and aconitase (ACO) as well as elevated ROS production. These alterations are most likely due to a loss of mitochondrial integrity. Cellular energy depletion and defect mitochondria elicit autophagy. In parallel mitochondrial dysfunction induces ER stress via activation of unfolded protein response. The disturbance of cellular energy generating pathways [mitochondrial (KC, Krebs cycle) and glycolytic (phosphofructokinase, PFK)] inhibits mTOR activity and, thereby, enhances autophagy. The interplay of ER stress and autophagy activates IL8 release.

of the University of Heidelberg. We received written informed consent for all cell lines included in this study.

Cell culture

Cells were prepared from urine of healthy donors ($n = 9$) and patients with mut^0 ($n = 5$) and cblB ($n = 1$) defects as well as patients affected with PAuria ($n = 3$) and purified tubular epithelial cells (hTEC). Primary epithelial cells of human proximal tubule were cultured in a selective medium containing Dulbecco's Modified Eagle Medium and Ham's F12 medium. It was supplemented with fetal calf serum, insuline, hydrocortisone, selenite, transferrin, hEGF, NAD and tri-iodo-thyronine. Confluent cells were subcultivated until 3rd passage and, subsequently, immortalized using pRSVneo vector containing SV40 DNA (pRNS1). Afterwards, immortalized tubular epithelial cells (hTEC) were characterized regarding morphology and protein expression.

Antibodies

The following antibodies were used for immunoblotting: rabbit polyclonal anit p-AMPK (sc-4778, Santa Cruz); mouse polyclonal anti-methylmalonylcoenzyme A mutase (#ab67869; Abcam, Camebridge, UK); rabbit polyclonal anti-aquaporin 1 (#AB2219; Millipore, Billerica, USA); rabbit polyclonal anti-aquaporin 2 (#A7310; Sigma, St. Louis, USA); sheep polyclonal anti-uromodulin (#K90071C; Meridian Life Science, Kampenhout, Belgium); mouse monoclonal anti-beta actin (#A5441; Sigma); rabbit polyclonal anti-sheep HRP (P0163; Dako, Glostrup, Denmark); goat polyclonal anti-rabbit HRP (P0488; Dako); goat polyclonal anti-mouse HRP (P0447; Dako); rabbit monoclonal anti p-IRE1 (#ab124945; Abcam); rabbit polyclonal anti LC3 (#L7543; Sigma, St Louis, USA); rabbit polyclonal anti p62 (#sc25575; Santa Cruz).

Immunoblotting

Immunoblotting was performed as previously described (33). Cells were cultivated until 80% confluence. Monolayers were collected in lysis buffer composed of 1 mM EDTA (Merck, Darmstadt, Germany), 20 mM imidazole (AppliChem GmbH, Darmstadt, Germany), 250 mM sucrose (VWR, Leuven, Belgium) containing protease inhibitors (Roche Diagnostics, Mannheim, Germany). Protein concentration was determined using Pierce BCA Protein Assay Kit (ThermoScientific, Rockford, USA). Samples [20 μg protein/lane] were diluted in Laemmli sample buffer (Bio-Rad, Hercules, CA, USA) and heated to 95°C for 6 min followed by sodium dodecyl sulfate (SDS) polyacrylamide gel electrophoresis (PAGE) and blotting on nitrocellulose membranes (Bio-Rad, Munich, Germany). Membranes were blocked 2 h at room temperature in non-fat dry milk (Bio-Rad, Hercules, CA, USA) followed by overnight incubation at 4°C with primary antibodies. After washing blots were incubated with peroxidase-conjugated secondary antibodies, washed again and visualized by Immun-Star enhanced chemiluminescence (Bio-Rad, Hempstead, UK). For quantitative analyses of western blots a FusionExpress system from peqlab was applied.

Mcm activity

Cells derived from human urine were classified as having mut^0 and cblB mutations by the assay of MCM activity. MCM activity was assayed in crude cell homogenates with (total MCM) and without (apo-MCM) the cofactor AdoCbl (50 mol/l) as described before (34).

Oxygen electrode

By using computer-supported high-resolution Oroboros 1 oxygraph system (Paar, Graz, Austria) mitochondrial respiratory rate was determined according to a previously described protocol (35). hTEC of controls and patients were placed in each electrode chamber. 'Mitochondrial respiratory rate (respiration-dependent ATP production)' was calculated by subtracting 'Background oxygen consumption rate (proton leak)' (recorded with a reference electrode in a presence of 10 μM NaCN) from 'Total oxygen consumption rate'.

Enzymes of cellular energy production

Activity of single enzyme complexes of electron transport chain, glycolysis and citrate cycle were recorded according to previously published protocols (12,36). A computer-tuneable spectrophotometer (Spectramax Plus Microplate Reader, Molecular Devices; Sunny Vale, CA, USA) operating in the dual wavelength mode was used. Measurement of the samples was performed in temperature-controlled 96-well plates in a final volume of 300 ml.

Radiometric analysis

Studies on the metabolism of ^{14}C-pyruvate and ^{14}C-2-oxoglutarate were performed according to previously published protocols (14).

Determination of ROS

Reactive oxygen species were measured by H_2DCFDA staining. Cells were stained with H_2DCFDA (10 μM) for 30 min. Then ROS generation was determined by FACS analysis (Canto II, Becton Dickinson).

Acridine orange staining

Cells were cultured in 6 cm petri dishes for 48 h in and, afterwards, incubated with acridine orange (1 μg/ml) colorless DMEM at 37°C for 20 min. Detection of green and red fluorescent cells was performed using a FACS system (Canto II, Becton Dickinson).

mTOR regulation

Regulation of mTOR signaling was analyzed using mTOR Regulation Antibody Sampler Kit (#9864; Cell Signaling) according to the manufacturer's protocol.

Determination of cytokines

To screen for changes in expression and secretion cytokines we used a Mix-N-Match ELISArray (SA Bioscience including IL8, MCP1, MIP-1a, MIP-1b, RANTES, TGF-ß) according to the manufacturer's protocol. IL-8 concentration was measured by enzyme-linked immunosorbent assay (ELISA) (Gen-probe, Eli-pair IL-8) again according to the manufacturer's protocol. For these experiments, hTEC were grown on 12-well TransWell filter plates for 48 h in standard medium. Thereafter, cells were washed twice with PBS and cultured in medium without FCS for 24 h. Then medium from the basolateral and apical site of well was collected, cells were harvested and medium and cell lysates were analyzed.

Electron micrographs

Cells were fixed with 1:1:1 (v/v) mixture of 0.05% ruthenium red (AppliChem; Darmstadt, Germany), 2.5% glutaraldehyde

(SERVA; Heidelberg, Germany) and cacodylate buffer, 2 h at RT. After washing with 0.2 M cacodylate buffer, cells were post-fixed with with 1:1:1 (v/v) of 0.05% ruthenium red, 0.2 M cacodylate buffer and 2% osmium tetroxide (Chempur; Karlsruhe, Germany) for 2 h at RT. Next, cells were washed with cacodylate buffer and dehydrated with serial ethanol concentrations (50, 80, 96 and 100%). Samples were embedded in Araldite (SERVA), contrasted with uranylacetate and lead citrate and sectioned with Ultracut 70 nm (Leica; Solms, Germany). Images were captured using EM 910 (Zeiss; Oberkochen, Germany).

Statistical analysis

Experiments were performed at least in triplicates. Data are analyzed using Mann–Whitney U tests for pairwise comparison and Kruskal–Wallis H test with subsequent Mann–Whitney U tests for multiple comparison (SPSS for Windows 16.0 Software).

Supplementary Material

Supplementary Material is available at *HMG* online.

Acknowledgements

Funding

References

1. Sniderman, L.C., Lambert, M., Giguere, R., Auray-Blais, C., Lemieux, B., Laframboise, R., Rosenblatt, D.S. and Treacy, E.P. (1999) Outcome of individuals with low-moderate methylmalonic aciduria detected through a neonatal screening program. *J. Pediatr.*, **134**, 675–680.
2. Fenton, W.A., Gravel, R.A. and Rosenblatt, D.S. (2001) Disorders of propionate and methylmalonate metabolism. In Scriver, C.R., Beaudet, A.L. and Valle, A.D. (eds) *The Metabolic and Molecular Bases of Inherited Disease*. McGraw-Hill, New York, pp. 2165–2193.
3. Brismar, J. and Ozand, P.T. (1994) CT and MR of the brain in disorders of the propionate and methylmalonate metabolism. *AJNR Am. J. Neuroradiol.*, **15**, 1459–1473.
4. Radmanesh, A., Zaman, T., Ghanaati, H., Molaei, S., Robertson, R.L. and Zamani, A.A. (2008) Methylmalonic acidemia: brain imaging findings in 52 children and a review of the literature. *Pediatr. Radiol.*, **38**, 1054–1061.
5. Hörster, F., Baumgartner, M.R., Viardot, C., Suormala, T., Burgard, P., Fowler, B., Hoffmann, G.F., Garbade, S.F., Kölker, S. and Baumgartner, E.R. (2007) Long-term outcome in methylmalonic acidurias is influenced by the underlying defect (mut0, mut-, cblA, cblB). *Pediatr. Res.*, **62**, 225–230.
6. Morath, M.A., Okun, J.G., Muller, I.B., Sauer, S.W., Horster, F., Hoffmann, G.F. and Kölker, S. (2008) Neurodegeneration and chronic renal failure in methylmalonic aciduria–a pathophysiological approach. *J. Inherit. Metab. Dis.*, **31**, 35–43.
7. Peters, H., Nefedov, M., Sarsero, J., Pitt, J., Fowler, K.J., Gazeas, S., Kahler, S.G. and Ioannou, P.A. (2003) A knock-out mouse model for methylmalonic aciduria resulting in neonatal lethality. *J. Biol. Chem.*, **278**, 52909–52913.
8. Manoli, I., Sysol, J.R., Li, L., Houillier, P., Garone, C., Wang, C., Zerfas, P.M., Cusmano-Ozog, K., Young, S., Trivedi, N.S. *et al.* (2013) Targeting proximal tubule mitochondrial dysfunction attenuates the renal disease of methylmalonic acidemia. *Proc. Natl. Acad. Sci. U. S. A.*, **110**, 13552–13557.
9. de Keyzer, Y., Valayannopoulos, V., Benoist, J.F., Batteux, F., Lacaille, F., Hubert, L., Chretien, D., Chadefeaux-Vekemans, B., Niaudet, P., Touati, G. *et al.* (2009) Multiple OXPHOS deficiency in the liver, kidney, heart, and skeletal muscle of patients with methylmalonic aciduria and propionic aciduria. *Pediatr. Res.*, **66**, 91–95.
10. Kimura, J., Ichii, O., Otsuka, S., Kanazawa, T., Namiki, Y., Hashimoto, Y. and Kon, Y. (2011) Quantitative and qualitative urinary cellular patterns correlate with progression of murine glomerulonephritis. *PLoS One*, **6**, e16472.
11. Schwab, M.A., Sauer, S.W., Okun, J.G., Nijtmans, L.G., Rodenburg, R.J., van den Heuvel, L.P., Drose, S., Brandt, U., Hoffmann, G.F., Ter Laak, H. *et al.* (2006) Secondary mitochondrial dysfunction in propionic aciduria: a pathogenic role for endogenous mitochondrial toxins. *Biochem. J.*, **398**, 107–112.
12. Kaminski, M.M., Sauer, S.W., Kaminski, M., Opp, S., Ruppert, T., Grigaravicius, P., Grudnik, P., Grone, H.J., Krammer, P.H. and Gulow, K. (2012) T cell activation is driven by an ADP-dependent glucokinase linking enhanced glycolysis with mitochondrial reactive oxygen species generation. *Cell Rep*, **2**, 1300–1315.
13. Nakano, M., Nakashima, A., Nagano, T., Ishikawa, S., Kikkawa, U. and Kamada, S. (2013) Branched-chain amino acids enhance premature senescence through mammalian target of rapamycin complex I-mediated upregulation of p21 protein. *PLoS One*, **8**, e80411.
14. Okun, J.G., Hörster, F., Farkas, L.M., Feyh, P., Hinz, A., Sauer, S., Hoffmann, G.F., Unsicker, K., Mayatepek, E. and Kölker, S. (2002) Neurodegeneration in methylmalonic aciduria involves inhibition of complex II and the tricarboxylic acid cycle, and synergistically acting excitotoxicity. *J. Biol. Chem.*, **277**, 14674–14680.
15. Kölker, S., Schwab, M., Horster, F., Sauer, S., Hinz, A., Wolf, N.I., Mayatepek, E., Hoffmann, G.F., Smeitink, J.A. and Okun, J.G. (2003) Methylmalonic acid, a biochemical hallmark of methylmalonic acidurias but no inhibitor of mitochondrial respiratory chain. *J. Biol. Chem.*, **278**, 47388–47393.
16. Kim, J., Devalaraja-Narashimha, K. and Padanilam, B.J. (2015) TIGAR regulates glycolysis in ischemic kidney proximal tubules. *Am. J. Physiol. Renal Physiol.*, **308**, F298–F308.
17. Chandler, R.J., Zerfas, P.M., Shanske, S., Sloan, J., Hoffmann, V., DiMauro, S. and Venditti, C.P. (2009) Mitochondrial dysfunction in mut methylmalonic acidemia. *FASEB J.*, **23**, 1252–1261.
18. Zsengeller, Z.K., Aljinovic, N., Teot, L.A., Korson, M., Rodig, N., Sloan, J.L., Venditti, C.P., Berry, G.T. and Rosen, S. (2014) Methylmalonic acidemia: a megamitochondrial disorder affecting the kidney. *Pediatr. Nephrol.*, **29**, 2139–2146.
19. Nulton-Persson, A.C. and Szweda, L.I. (2001) Modulation of mitochondrial function by hydrogen peroxide. *J. Biol. Chem.*, **276**, 23357–23361.
20. Kalyanaraman, B., Darley-Usmar, V., Davies, K.J., Dennery, P.A., Forman, H.J., Grisham, M.B., Mann, G.E., Moore, K., Roberts, L.J. 2nd. and Ischiropoulos, H. (2012) Measuring reactive

oxygen and nitrogen species with fluorescent probes: challenges and limitations. *Free Radic. Biol. Med.*, **52**, 1–6.

21. Kimura, T., Takahashi, A., Takabatake, Y., Namba, T., Yamamoto, T., Kaimori, J.Y., Matsui, I., Kitamura, H., Niimura, F., Matsusaka, T. *et al*. (2013) Autophagy protects kidney proximal tubule epithelial cells from mitochondrial metabolic stress. *Autophagy*, **9**, 1876–1886.

22. Rogov, V., Dotsch, V., Johansen, T. and Kirkin, V. (2014) Interactions between autophagy receptors and ubiquitin-like proteins form the molecular basis for selective autophagy. *Mol. Cell*, **53**, 167–178.

23. Inoki, K. (2014) mTOR signaling in autophagy regulation in the kidney. *Semin. Nephrol.*, **34**, 2–8.

24. Parrales, A., Lopez, E., Lee-Rivera, I. and Lopez-Colome, A.M. (2013) ERK1/2-dependent activation of mTOR/mTORC1/p70S6K regulates thrombin-induced RPE cell proliferation. *Cellular Signalling*, **25**, 829–838.

25. Copp, J., Manning, G. and Hunter, T. (2009) TORC-specific phosphorylation of mammalian target of rapamycin (mTOR): phospho-Ser2481 is a marker for intact mTOR signaling complex 2. *Cancer Res.*, **69**, 1821–1827.

26. Jung, C.H., Jun, C.B., Ro, S.H., Kim, Y.M., Otto, N.M., Cao, J., Kundu, M. and Kim, D.H. (2009) ULK-Atg13-FIP200 complexes mediate mTOR signaling to the autophagy machinery. *Mol. Biol. Cell*, **20**, 1992–2003.

27. Ganley, I.G., Lam du, H., Wang, J., Ding, X., Chen, S. and Jiang, X. (2009) ULK1.ATG13.FIP200 complex mediates mTOR signaling and is essential for autophagy. *J. Biol. Chem.*, **284**, 12297–12305.

28. Kato, H., Nakajima, S., Saito, Y., Takahashi, S., Katoh, R. and Kitamura, M. (2012) mTORC1 serves ER stress-triggered apoptosis via selective activation of the IRE1-JNK pathway. *Cell Death Differ.*, **19**, 310–320.

29. Shanware, N.P., Bray, K., Eng, C.H., Wang, F., Follettie, M., Myers, J., Fantin, V.R. and Abraham, R.T. (2014) Glutamine deprivation stimulates mTOR-JNK-dependent chemokine secretion. *Nat. Commun.*, **5**, 4900.

30. Benbrook, D.M. and Long, A. (2012) Integration of autophagy, proteasomal degradation, unfolded protein response and apoptosis. *Exp. Oncol.*, **34**, 286–297.

31. Segerer, S., Henger, A., Schmid, H., Kretzler, M., Draganovici, D., Brandt, U., Noessner, E., Nelson, P.J., Kerjaschki, D., Schlondorff, D. *et al*. (2006) Expression of the chemokine receptor CXCR1 in human glomerular diseases. *Kidney Int.*, **69**, 1765–1773.

32. Wrobel, L., Topf, U., Bragoszewski, P., Wiese, S., Sztolsztener, M.E., Oeljeklaus, S., Varabyova, A., Lirski, M., Chroscicki, P., Mroczek, S. *et al*. (2015) Mistargeted mitochondrial proteins activate a proteostatic response in the cytosol. *Nature*, **524**, 485–488.

33. Wang, S.S., Devuyst, O., Courtoy, P.J., Wang, X.T., Wang, H., Wang, Y., Thakker, R.V., Guggino, S. and Guggino, W.B. (2000) Mice lacking renal chloride channel, CLC-5, are a model for Dent's disease, a nephrolithiasis disorder associated with defective receptor-mediated endocytosis. *Hum. Mol. Genet.*, **9**, 2937–2945.

34. Baumgartner, E.R. (1983) Activity of the cobalamin-dependent methylmalonyl-CoA mutase. In Hall, C.A. (ed), *The Cobalamins, Methods in Hematology*, Churchill Livingston, Edinburgh, New York, 10, pp. 181–195.

35. Heerlein, K., Schulze, A., Hotz, L., Bartsch, P. and Mairbaurl, H. (2005) Hypoxia decreases cellular ATP demand and inhibits mitochondrial respiration of a549 cells. *Am. J. Respir. Cell Mol. Biol.*, **32**, 44–51.

36. Sauer, S.W., Okun, J.G., Schwab, M.A., Crnic, L.R., Hoffmann, G.F., Goodman, S.I., Koeller, D.M. and Kölker, S. (2005) Bioenergetics in glutaryl-coenzyme A dehydrogenase deficiency: a role for glutaryl-coenzyme A. *J. Biol. Chem.*, **280**, 21830–21836.